

# Magnetic Properties and Crystallization Kinetics of a Mn-Doped FINEMET Precursor Amorphous Alloy

A. C. Hsiao, M. E. McHenry, D. E. Laughlin, M. R. Tamoria, and V. G. Harris

**Abstract**—The kinetics of nanocrystallization of a Mn-doped FINEMET alloy from its amorphous precursor is reported. The alloy studied was of a composition  $(\text{Fe}_{1-x}\text{Mn}_x)_{73.5}\text{Nb}_3\text{CuSi}_{13.5}\text{B}_9$  where  $x = 0.05$ . X-ray diffraction (XRD) confirmed that  $\alpha$ -FeSi is the product of primary nanocrystallization. Crystallization kinetics were studied using time-dependent magnetization,  $M(t)$ , as a measure of the volume fraction crystallized. This data was taken using vibrating sample magnetometry (VSM) and thermal analysis employing differential scanning calorimetry (DSC). Primary crystallization for the Mn-doped FINEMET alloy was found to occur at 505 °C, for DSC data taken at a heating rate of 10 °C/min. Fits to the Kissinger equation for constant heating transformations yield an activation energy for crystallization of 3.4 eV. VSM measurements of isothermal  $M(t)$  show that the maximum volume fraction transformed was reached at 20 min. Measurements of magnetic anisotropy as a function of time probe the structural evolution of the material upon nanocrystallization. Measurements show stress relaxation occurring at 20 minutes at 490 °C, coinciding with the maximum volume fraction crystallized.

**Index Terms**—Crystallization kinetics, magnetic anisotropy, magnetization vs. time, Mn-doped FINEMET.

## I. INTRODUCTION

FINEMET™ is an amorphous/nanocrystalline nanocomposite soft ferromagnetic material that has been suggested for such magnetic components as saturable reactors, choke coils, and transformers. Here we report the nanocrystallization kinetics of the amorphous precursor to a Mn-doped FINEMET alloy. The study of crystallization kinetics of amorphous precursors to nanocrystalline soft magnets contributes to the understanding of microstructural development and its influence on soft magnetic properties. FINEMET was one of the first amorphous/nanocrystalline ferromagnetic nanocomposites to be synthesized, studied and eventually commercialized (Yoshizawa *et al.* [1]). The soft magnetic properties of FINEMET result from its two phase nanocomposite microstructure where nanocrystalline grains of an  $\alpha$ -Fe-Si phase is embedded in the amorphous matrix. This fine microstructure

has been shown to depend on Cu atoms (which are not soluble in BCC-Fe or the derivative DO<sub>3</sub> structure of  $\alpha$ -Fe-Si) clustering and aiding nucleation for nanocrystallization of Fe-Si grains [2], [3].

Previously reported thermomagnetic data for FINEMET show that the Curie temperature ( $T_c$ ) for the amorphous phase is 280 °C and the onset of crystallization occurs at  $\sim$ 490 °C. At this point a ferromagnetic nanophase begins to form in the paramagnetic amorphous matrix. The ferromagnetic to paramagnetic transition of the Fe-Si nanocrystallites occurs at  $T_{c(\text{Fe,Si})} = 630$  °C [4].

Mn doping of FINEMET is aimed at investigating the partitioning of a small amount of a different magnetic transition metal (Mn) between iron-silicon ( $\alpha$ -Fe-Si) nanocrystals and the intervening amorphous phase. The doping of manganese into  $\alpha$ -Fe-Si nanocrystals may serve to expand the Fe-Si lattice and potentially increase the Fe magnetic moment. On the other hand, since exchange is sensitive to interatomic distance, the Curie temperature of the amorphous precursor, the  $\alpha$ -FeSi nanocrystals, and the intervening amorphous phase may all be altered by Mn additions. Partitioning of Mn and exchange coupling effects are discussed in a companion paper in this volume.

Previous magnetic and nanocrystallization work reported in literature for FINEMET doped with chromium (Cr) has been reported by A. Slawska-Waniewska *et al.* [5]. The addition of Cr results in a slight stabilization of the amorphous alloy against nanocrystallization, thus increasing the crystallization temperature of the material ( $T_x$ ). The addition of increasing amounts of Cr also results in a decrease in the Curie temperature ( $T_c$ ) of the amorphous phase and a slightly smaller nanocrystalline grain size [6].

## II. PROCEDURE

Amorphous ribbon precursors of Mn-doped FINEMET with the composition  $(\text{Fe}_{1-x}\text{Mn}_x)_{73.5}\text{Nb}_3\text{CuSi}_{13.5}\text{B}_9$  where  $x = 0.05$  were prepared by melt-spinning at the Naval Research Laboratory. The sample dimensions were 2–3 mm in width and 20–30  $\mu\text{m}$  thick. After nanocrystallization DSC measurements of the temperature of crystallization ( $T_x$ ) were performed at five different rates: 10 °C/min, 15 °C/min, 30 °C/min, 50 °C/min, and 70 °C/min. VSM measurements of the isothermal magnetization as a function of time were made to observe nanocrystallization kinetics near  $T_x$ . Additional measurements of magnetic properties as a function of time on the VSM include that of the saturation magnetization ( $M_s$ ), magnetic anisotropy, and coercive field ( $H_c$ ). The VSM was also used to measure magnetization as a function of applied field.

Manuscript received October 13, 2000.

This work was supported by the National Science Foundation through Grant Award DMR-9803700, and also from the Air Force Office of Scientific Research, Air Force Material Command, USAF, under Grant F49620-96-1-0454, and from ABB Corporation. The work of M. R. Tamoria and V. G. Harris was supported by the Office of Naval Research.

A. C. Hsiao, M. E. McHenry, and D. E. Laughlin are with the Department of Materials Science and Engineering at Carnegie Mellon University, Pittsburgh, PA 15213 USA (e-mail: mm7g@andrew.cmu.edu).

M. R. Tamoria and V. G. Harris are with the Naval Research Laboratory, Code 6342, Washington, DC 20375 USA (e-mail: harris@anvil.nrl.navy.mil).

Publisher Item Identifier S 0018-9464(01)06563-3.

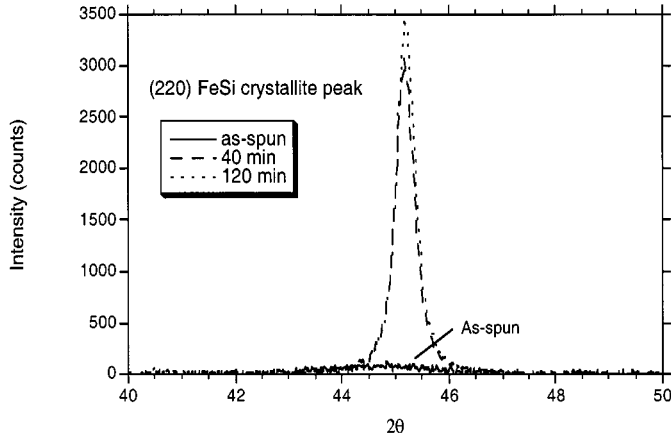


Fig. 1. XRD data measuring intensity as a function of  $2\theta$ . The graph indicates that FeSi is the first phase to crystallize from the amorphous phase. Bragg peaks are not detected for as-spun Mn-doped FINEMET indicating that it is fully amorphous. The intensity for peaks for the sample annealed for 120 min. is sharper and more narrow than the sample annealed for 40 min.

### III. RESULTS AND DISCUSSION

#### A. X-Ray Diffraction

Fig. 1 shows the x-ray diffraction patterns for Mn-doped FINEMET measured as-spun, annealed at  $490^\circ\text{C}$  for 40 min, and annealed at  $490^\circ\text{C}$  for 120 min. The XRD pattern is indexed to the  $\text{D0}_3$  lattice of the FeSi unit cell, which is twice that of the BCC-Fe unit cell. The XRD data confirms that FeSi is the first phase to nanocrystallize from the amorphous matrix. The sharpness of the intensity peaks increases with annealing time (signifying some coarsening of the grains). This can be seen in the (220) peak and indicates increased crystallinity. Scherrer analysis confirms that the particle size is 7 nm for the sample annealed for 120 min. and 4 nm for the sample annealed for 40 min.

#### B. Kissinger Model of Crystallization Kinetics

The crystallization temperature  $T_x$  of Mn-doped FINEMET was measured by DSC using a Kissinger model of kinetics for various heating rates. For Mn-doped FINEMET,  $T_x$  was found to be  $505^\circ\text{C}$  at  $10^\circ\text{C}/\text{min}$  from the DSC exothermic peak. The Kissinger equation:

$$\ln\left(\frac{\alpha}{T_x^2}\right) = -\frac{Q_K}{RT_x} + \text{constant} \quad (1)$$

relates the natural log of the heating rate ( $\alpha$ ) and the square of the crystallization temperature ( $T_x$ ) to the activation energy ( $Q_K$ ), the ideal gas constant ( $R$ ) and  $T_x$ . The activation energy,  $Q_K$ , is determined from the slope of the line between  $\ln(\alpha/T_x^2)$  vs.  $1/(T_x * 10^3)$  as shown in Fig. 2. For our alloy,  $Q_K$  is calculated to be 3.4 eV. This value is comparable to the experimental values for undoped FINEMET of 3.7–4.5 and 3.8 eV, as reported by L. K. Varga [7] and Conde [8], respectively.

#### C. Magnetic Measurements of Crystallization Kinetics

The Johnson–Mehl–Avrami (JMA) model for crystallization kinetics using isothermal heating can be used to describe the magnetization as a function of time in the nanocrystallization

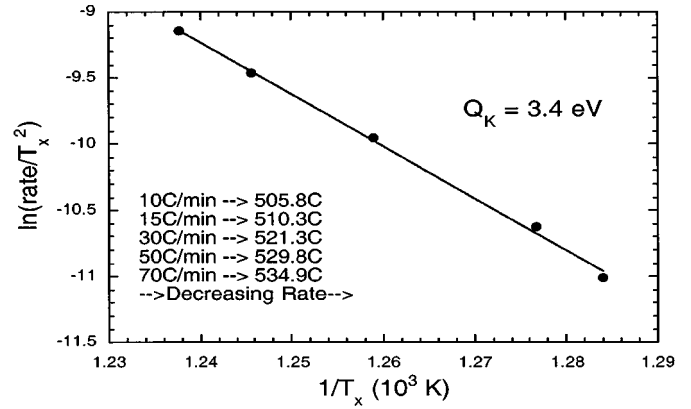


Fig. 2. Kissinger plot for Mn-doped FINEMET. The plot shows a linear fit to the the Kissinger equation from DSC heating rate experiments. The crystallization temperature  $T_x$  is dependent upon heating rate. The activation energy  $Q_K$  of the transformation, calculated from the slope of the plot, is 3.4 eV.

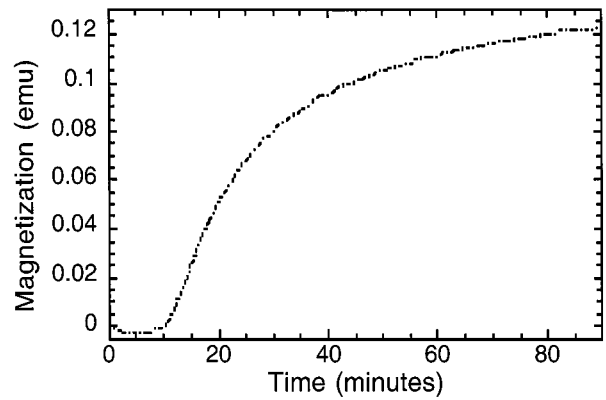


Fig. 3. Magnetization vs. time as measured by VSM. The sample was heated at  $490^\circ\text{C}$ , slightly below  $T_x = 505^\circ\text{C}$ . An incubation time of  $\sim 5$ – $10$  min. is observed. The inflection point of this curve, i.e., maximum  $dM/dt$ , is directly proportional to the maximum rate of transformation,  $dX/dt$ .

of Mn-doped FINEMET as shown in Fig. 3. Since the Curie temperature,  $T_c$ , of the amorphous phase is lower than the crystallization temperature,  $T_x$ , in FINEMET, the crystallization results in a magnetic phase evolving from a nonmagnetic phase. Therefore, the volume fraction transformed is proportional to the magnetization. The measure of the rate of transformation,  $dM/dt$ , has a maximum when  $\sim 50\%$  of the transformation has occurred. As nanocrystallization occurs from the amorphous matrix, the magnetization of the 2-phase sample increases until the material is fully crystallized, reaching saturation magnetization. The inflection point of the  $M$ . vs.  $t$  curve reveals the time during the transformation at which the maximum rate of transformation occurs. This time is measured to be  $\sim 20$  minutes for Mn-doped FINEMET. The saturation of  $M$  vs.  $t$  at  $490^\circ\text{C}$  indicates the end of primary crystallization, not that the sample has fully crystallized.

#### D. Magnetic Properties with Structural Evolution

The evolution of magnetic properties is well correlated with the structural evolution that occurs during nanocrystallization. As shown in Fig. 4, a slight softening occurs before nanocrystallization due to the relaxation of internal stresses within the

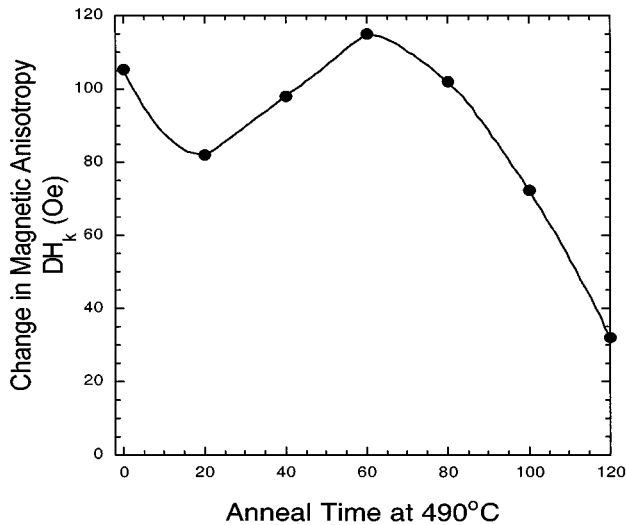


Fig. 4. Change in magnetic anisotropy vs. anneal time at 490 °C. Stress relaxation occurs at 20 minutes, corresponding to the time of the maximum rate of transformation.

amorphous matrix. This softening is observed as a decrease in magnetic anisotropy immediately before the maximum rate of transformation. This change in anisotropy field is induced by aging. The baseline anisotropy field, dominated by shape anisotropy, was measured by VSM. Similarly, at the start of crystallization, the crystalline fraction is very low and the average distance between the crystallites is longer than the exchange correlation length in the amorphous matrix. Therefore the distant ferromagnetic grains are not strongly exchange coupled. Instead the crystallites act as pinning centers for domain walls in the amorphous matrix and allow magnetic hardening to occur. This magnetic hardening is observed as an increase in coercivity in the early stages of nanocrystallization. As annealing time increases, the distance between nanocrystallites and the effect of interactions with the amorphous phase decreases. A similar two-phase model with changes in coercivity

and magnetic anisotropy during nanocrystallization has been investigated by Hernando *et al.* [10] as an extension to the Herzer model.

#### IV. CONCLUSION

The magnetic properties and crystallization kinetics of Mn-doped FINEMET were studied. An essential feature of FINEMET-type nanocrystalline materials is its two-phase amorphous-nanocrystalline character that remains until its second crystallization temperature. Time dependent magnetization is a technique that can be used to probe microstructural changes that correlate with magnetic changes at the onset of and during nanocrystallization. Stress relaxation as observed by the change in magnetic anisotropy correlated with the volume fraction of nanocrystallites transformed, as measured by magnetization over time. The Kissinger and Johnson–Mehl–Avrami models of crystallization kinetics both contribute to the understanding of crystallization kinetics and the activation energy of reactions. The values of  $Q_K$  and  $Q_{JMA}$  are comparable [9].

#### REFERENCES

- [1] Y. Yoshizawa, S. Oguma, and K. Yamauchi, *J. Appl. Phys.*, vol. 64, p. 6044, 1988.
- [2] J. D. Ayers, V. G. Harris, J. A. Sprague, W. T. Elam, and H. N. Jones, *Acta Mater.*, vol. 46, no. 6, pp. 1861–1874, 1998.
- [3] K. Hono, K. Hiraga, Q. Wang, A. Inoue, and T. Sakurai, *Acta Metall. Mater.*, vol. 40, no. 9, pp. 2137–2147, 1992.
- [4] For a review see M. E. McHenry, M. A. Willard, and D. E. Laughlin, *Prog. Mat. Sci.*, vol. 44, p. 291, 1999.
- [5] A. Slawska-Waniewska, M. Gutowski, and H. K. Lachowicz, *Phys. Rev. B*, vol. 46, pp. 14 594–14 597, 1992.
- [6] V. Franco, C. F. Conde, and A. Conde, *J. Magn. Magn. Mater.*, vol. 203, pp. 60–62, 1999.
- [7] L. K. Varga, *Mat. Sci. and Eng.*, vol. A179/A180, p. 567, 1994.
- [8] C. F. Conde and A. Conde, *Mat. Lett.*, vol. 21, p. 409, 1994.
- [9] A. Hsiao, Z. Turgut, M. A. Willard, E. Selinger, D. E. Laughlin, M. E. McHenry, and R. Hasegawa, *MRS Symp. Proc.*, vol. 577, 1999, pp. 551–556.
- [10] A. Hernando, M. Vazquez, T. Kulik, and C. Prados, *Phys. Rev. B*, vol. 51, p. 3581, 1995.